

A PREDICTIVE MODEL FOR THE ASSESSMENT OF AGGREGATE SENSITIVITY TO ASR

Mario Kositz and Klaus-Juergen Huenger

Biography: **Mario Kositz** is a scientific assistant at the Brandenburg University of Technology Cottbus - Senftenberg. He is a coworker of the chair Building materials and Building Chemistry. He received his MS from the university in Cottbus in 2009. His research interests include assessment of ASR aggregate reactivity, modeling for ASR prediction and durability of concrete structures in the field of structural engineering.

Klaus-Juergen Huenger is leader of the chair Building Materials and Building Chemistry at the Brandenburg University of Technology Cottbus - Senftenberg. He received his PhD from the Bauhaus University in Weimar in 1989 and his habilitation from the University of Cottbus in 2005. His research interests include damaging processes in the whole field of structural engineering.

ABSTRACT

Different aggregates stored in alkaline solutions have different solubility of silica and alumina. The dissolved silica reacts with water and alkalis to form an alkali silica gel, which can swell. ASR swelling can be reduced or prevented, if enough space is available for the alkali silica gel formation. This “space” is the open porosity, which can also be determined directly at the aggregate grains.

Concrete specimens made with different aggregates were produced. They all were stored in a fog chamber at 104°F (40°C) and the ASR swelling was measured for one year. At the same time, the aggregates were stored in 0.1 mol KOH solution at 176°F (80°C) for 56 d only. The solubility of silica and alumina was determined continuously by ICP-OES.

The obtained dissolution rates, open porosity and expansion data were compared and a reliable model for predicting the ASR sensitivity of concrete aggregates was derived.

Keywords: alkali silica reaction, modeling, aggregate reactivity, dissolution of silica and alumina, dissolution rate, open porosity

INTRODUCTION

At this moment, several test methods to classify aggregate sensitivity to ASR (Alkali-Silica-Reaction) are available. Usually concrete specimens are produced, and the expansion against time is measured. After a certain time the expansion is compared with a limit value. If the limit has been exceeded, the aggregate is classified as sensitive to ASR. In the other case, it will be resistant or non-sensitive to ASR.

These test methods are standardized (e.g. AMBT & CPT) in Germany, and international several standards are available. Therefore, the storing temperature and humidity and time, water/cement ratio (w/c), amount of cement, cement type, OH^- concentration of the cement paste, volume fraction and grading curves of the aggregate worldwide differ. Because of this, the characterizations of the ASR sensitivity are not comparable.

An alternative test for aggregates (adapted to the CPT) was developed by Hill [1] in 2004. An aggregate chemical quick test called “BTU-Test” (named after Brandenburg University of Technology in Cottbus) includes the dissolution of silica and alumina. The crushed and ground

aggregates are stored in 0.1 molar KOH at 176°F (80°C). The “excess silica” value for the available SiO₂ for ASR (1) was defined as:

$$SiO_{2exc} = SiO_{2soluble} - 1.4 Al_2O_3 \quad (\text{in mg/L}). \quad (1)$$

Huenger [2] and Chappex and Scrivener [3] show the significant role of alumina in several kinds of greywacke rocks. This equation (1) is based on the result, that the other part of soluble SiO₂ is bound to innocuous aluminosilicate structures by the dissolved alumina. Depending on the proportion of silica and alumina in the solution, there are two codomains possible:

SiO_{2soluble} > 1.4 Al₂O₃ & SiO_{2exc} > 0 available SiO₂ for ASR
 SiO_{2soluble} ≤ 1.4 Al₂O₃ & SiO_{2exc} ≤ 0 complete aluminosilicate formation or excess of Al, ASR improbable

If the BTU-Test is used, the test duration decreases to only 14d.

A further development has been done by Bachmann [4]. Bachmann improved or better extended the BTU-Test and takes the open porosity of the aggregate grains into account. The test was expanded to more aggregate types like gravels, rhyoliths etc. **Fig. 1.** shows that the ASR reactivity depends on the SiO_{2exc} value at the age of 14d and the open porosity. Three cases are possible:

$SiO_{2exc} \leq 4.56E-02 \text{gr/fl oz (100mg/L)}$	means the aggregate is innocuous
$4.56E-02 \text{gr/fl oz} \leq SiO_{2exc} < 1.83E-01 \text{gr/fl oz (400mg/L)}$	the aggregate reactivity depends on the volume of open porosity
$1.83E-01 \text{gr/fl oz (400mg/L)} \geq SiO_{2exc}$	the aggregate is sensitive to ASR, the porosity could not reduce the ASR potential

Kronemann [5] invented the “modified BTU-test” and compared the rate of aggregate dissolution in highly alkaline solutions with the expansion curves of the German CPT [6]. Kronemann used uncrushed aggregate grains with their original size and increased the aggregate sample amount to 0.198lb (90g). The samples are stored in 0.1m KOH at 176°F (80°C) for 56d. The amount of silica and alumina was measured by ICP-OES and the derivation SiO_{2exc} after time was calculated. **Fig. 2** shows the detailed procedure. The investigation time increases from 14d (BTU-SP Test) to 56d (mod. BTU-Test) because of the lower grain surface area. The dissolution time of 56d corresponds to 273d of the CPT. The process was divided into four time periods. Every time step corresponds to a special phase of ASR.

- 0-4 days innocuous to ASR, because of cement paste hydration
- 4-14 days beginning of ASR
- 14-28 days mid age of ASR, the ASR is in full progress
- 28-56 days end of ASR, the ASR velocity decreases.

Fig. 3 shows SiO_{2exc}/dt results of two aggregates. On the left side a highly sensitive greywacke is shown with rates of $SiO_{2exc}/dt > 1.60E-02 \text{gr/(fl oz*d)} (35 \text{mg/[L*d]})$ in every phase. And on the right side, a non sensitive andesite can be seen with rates smaller than $2.28E-03 \text{gr/(fl oz*d)} (5 \text{mg/[L*d]})$. Although the porosity was neglected, a good qualitative correlation was found to classify aggregates.

Various kinds of ASR models have been published in recent years. Most of them consider the concrete mixture design, and include the porosity, silica content and crack propagation for already existing structures [7]. The calculations starts after the building showed an ASR deterioration. Santos et al. [8] showed the ability for calculating the deflection of ASR dams, which are large damaged. Real predictive models for the assessment of ASR reactivity, determined directly at the aggregates, are not discussed.

The modified BTU-Test method should be developed further to achieve a faster characterization by using a model approach.

RESEARCH SIGNIFICANCE

The reliable ASR risk assessment (e.g. CPT) needs effort, costs, investigation time and large concrete specimens. However, test durations above nine months are not purposeful for the aggregate industry.

Chemical aggregate tests can significantly reduce the investigation time (compared to the CPT) and increase the reliability. Additionally it will be possible to compare different rocks. Furthermore, most test methods differentiate between white (innocuous) and black (reactive) aggregates. Until now, there is no “grey” classification possible [6]. The procedural errors of the modified BTU-test are much lower than the errors of any expansions test. This allows precise statements to ASR sensitivity.

EXPERIMENTAL INVESTIGATION

In order to determine the correlation between the dissolution rates and the expansion graphs, four types of experiments were performed. First the concrete bar specimens were produced and expansions were measured according to the German alkali-guideline [6]. The silica and alumina dissolution of the aggregates were measured with ICP-OES. The open porosity of the aggregates was determined by water adsorption [9].

Materials

The test matrix contained altogether eighteen different aggregate types with grain sizes 0.08/0.31 (2/8mm) & 0.31/0.63 (8/16mm). The chosen aggregates consisted of greywacke, andesite, rhyolite, natural rounded gravel and crushed gravel (**Table 1** and **Fig. 4**). Because of that, it is possible to discuss the influence of crushing. For all eighteen aggregates, the weighted aggregate fraction 0.08/0.31 (2/8) and 0.31/0.63 (8/16) corresponds to the grading curve A/B16 according to the European standards. The concrete mixtures contained an ASR innocuous sand 0/0.078 (0/2mm). The sand shows a very low SiO_{2exc} dissolution behavior which will not be shown here. The alkali equivalent of the ordinary portland cement (**Table 2**) was boosted to 1.30 wt.-% by adding K_2SO_4 (0.605 wt.-% relatively to the testing cement content) to the mixing water. This procedure is prescribed by the alkali guideline [6]. The SO_3 content of cement increases a little bit from 3.07% to 3.25%. Because all influences have kept constant, a possible ASR expansion can only be attributed to the different aggregates used.

The solution for the solubility experiments contains 0.1m KOH/L prepared from analytical grade materials.

Specimens

For each aggregate three concrete bar specimens (3.94 in. [100 mm] width/height and 21.65 in. [550 mm] length) are necessary for the ASR sensitivity assessment. The standard concrete mixture is shown in **Table 3**. The concrete specimens were cast and stored in the fog chamber

at 104°F (40°C) with at least 98% RH for 365d. The expansion was measured periodically, prescribed in [6].

The dissolution experiments were performed with 0.198lb (90g) aggregate in the original particle size and 1.98lb (900g) 0.1m KOH solution. The samples were placed in tightly sealed polyethylene bottles at 176°F (80°C). After 4, 14, 28, and 56 days, respectively, approx. 0.10fl oz (3ml) of solution were taken from the liquid phase, filtered through a 5.67E-04p (0.2µm) membrane filter and analyzed by ICP-OES. In the alkaline solutions obtained by the dissolution experiments, the concentrations of dissolved Si ($\lambda_{Si}=251.611\text{nm}$) and Al ($\lambda_{Al}=396.152\text{nm}$) were determined. The aim of this paper is to show the interaction between the dissolution rates and the ASR induced expansion of different aggregates.

ANALYTICAL INVESTIGATION

The velocity of the expansion is calculated by eq. 2. It contains the chemical part SiO_{2exc} and a dimensionless form factor S . The dissolution of SiO_{2exc} is being considered as an independent variable, which has an accelerating or decelerating character.

$$\frac{d\varepsilon_{ASR}}{dt} = \frac{dS}{dt} * \frac{dSiO_{2exc}}{dt} \quad (2)$$

ε_{ASR} = ASR expansion in %
 S = shape function
 SiO_{2exc} = excess silica value

Based on the four ASR phases by Kronemann [5], a form function (S) with variable speed steps is needed. Former investigations showed that every expansion graph has a shape of an evolutionary- or sigma function. It represents a slow speed in the beginning, the maximum speed by reaching the point in inflection and a decreasing speed until reaching the maximum value (**Fig. 5**). The same phenomena was found decades ago analyzing the hydration process of OPC [10,11,12]. Multiple continuous speed steps like Kronemann [5] can be achieved by using the autonomous differential equation (3).

$$S' = f(S) = k_1 * \left(\frac{S}{S_I}\right)^m * \left(\frac{S_\infty - S}{S_\infty - S_I}\right)^n \quad \text{with } S(0) = 1E - 08 \text{ L * d/mg} \quad (3)$$

S = shape function
 k_1 = maximum speed constant for each aggregate (see Fig. 10)
 S_I = point of inflection for each aggregate (point on the x-axis, where k_1 occurs, see Fig. 11)
 S_∞ = maximum value (maximum point of each curve on the x-axis, see Fig. 11)
 m, n = constants which represents the leaning of the shape or the rise the at S_I

In the next step, until now, we do not know whether k_1 , S_I and S_∞ are functions too. These parameters are still unknown. However the experimental results of the solubility, porosity and the expansion of eighteen aggregates are available, and the unknown values need to be determined. With a fourth order Runge-Kutta [13] method the equation (3) can be solved numerically. The estimation of the parameters is based on the randomly stochastic value search, in which the quality of the adjustment is calculated by using the least squared method. For all aggregates 90 parameters (18 x 5) have to be identified. The chosen equations describe a nonlinear, crack free and elastic material behavior.

The expansions of the CPT according to the German alkali-guideline [6] include parts of thermal, moisture and of course the ASR-expansion. The 18 aggregates showed different thermal and moisture expansions after 28d. The assumption is that ASR is a really slow process. Even under tropical climate conditions (e.g. fog chamber) ASR expansion will not occur before the age of 28d. Because of this, all expansion graphs are adjusted to zero at the 28d starting point. This fact differs bit from [6]. But during the calculation it was shown that the ASR expansion will be more homogeneous for all rocks. By using a special heater and ultrasound moisture controller, the humidity and the temperature could be kept constant everywhere in the fog chamber. This was necessary to avoid a temperature gradient between the lowest and the highest shelves.

EXPERIMENTAL RESULTS AND DISCUSSION

Open porosity

With the pycnometer method [9] the aggregate density, water adsorption and open porosity was determined together. The results of the open porosity are shown in **Fig. 6**. It can be seen that the porosity varies from 1.40 (agg.1) until 5.40 vol.-% (agg.7). The values for all other rock materials and all other aggregates are located in this range. It seems, that the grain size fraction 0.08/0.31 (2/8) have always the same or higher porosity than 0.31/0.63 (8/16). Aggregate 13 as a rounded gravel shows higher porosity than the crushed one (agg.12). The same fact can be seen by taking agg.16 and agg.17. Crushing an aggregate decreases the available open porosity.

Solubility of aggregates

In **Fig. 7** the solubilities of the grain sizes 0.08/0.31 (2/8) and 0.31/0.63 (8/16) are documented, where the values are weighted according to the volume fraction of the CPT.

The aggregates show a different SiO_{2exc} solubility behavior. Aggregate 7 gives nearly no SiO_{2exc} into the solution. The solubility graph seems to be linear from 0-56d. Aggregate 13 reaches 0.30gr/fl oz (750mg/L) at the age of 14d and then the dissolution rate decreases. At the age of 56d agg.13 shows a solubility of 0.55gr/fl oz (1200mg/L). The crushed aggregate 12 has the same solubility until 14d, but then it increases further and leads to 0.75gr/fl oz (1600mg/L) after 56d. Like aggregate 13, the speed decreases after 14d. After 56d the greywacke (agg.4) dissolves more than 1.20gr/fl oz (2500mg/L) SiO_{2exc} into the alkaline solution. Its dissolution graph seems to be linear like agg.7. The quartzite aggregate 5 shows the highest SiO_{2exc} solubility. After 56d storage, nearly 1.80gr/fl oz (4000mg/L) was detected.

In **Fig. 8** the calculated SiO_{2exc} rates are shown. Aggregate 7 (andesite) shows values smaller than $2E-03$ gr/(fl oz*d) (5 mg/[L*d]). The quartzite (agg.5) reaches a velocity about $6E-02$ gr/(fl oz*d) (100 mg/[L*d]). The influence of crushing can also be seen. The rounded gravel (agg.13) shows lower rates than the crushed one (agg.12). The same can be adopted to aggregate 16 and 17. Therefore, the SiO_{2exc} solubility increases if an aggregate is being crushed.

CPT expansions

Fig. 9 shows the experimental expansion results of the CPT. All aggregates show different behaviors. The agg.7 shows nearly no expansion (ca. $9.0E-03\%$) due to ASR, the greywacke agg.4 leads to $2.0E-01\%$. The gravel agg.17 reaches with $1.3E-01\%$ its maximum. Aggregate 16 shows an expansion of $3.0E-02\%$ after 180 d. Although both gravels consist of the same material, the effect of crushing increases, obviously, the ASR sensitivity. The same behavior is shown by gravel 12 and 13. How expected, all CPT expansion graphs have an evolutionary shape.

COMPARISON OF PREDICTIONS AND EXPERIMENTAL RESULTS

After smoothing the experimental data, the regression analysis shows an average degree of certainty about 98.6%. For an ASR as a multi-influenced and complicated process (especially the occurrence of cracks), this is a quite good value. The chemical constants were found and varied between $n = 1.08 \pm 0.08$ and $m = 0.78 \pm 0.11$ for all eighteen equations.

Fig. 10 shows dS/dt (based on eq. 2 by changing) against time. Here the function dS/dt involves the velocity of $S(t)$. It can be seen that every aggregate has a different maximum velocity (k_1). The greywacke (agg.4) has the largest value $3.4E-07$ 1/d at the age of 70 d. The crushed aggregate 17 reaches $3.0E-07$ 1/d at 74 d. The rounded gravel (agg.16) shows $5.2E-08$ 1/d at 105 days. The maximum velocity of every aggregate occurs at a different time. At this moment, the forced diffusion and reaction period (eq. 3) can be seen.

In **Fig. 11** the velocity dS/dt against $S(t)$ is plotted. The curves start in the origin and begin to increase. The maximum y-value of each curve represents the value k_1 . The x-value of k_1 is S_I from (2). After leaving the top, the speed decreases, and when it hits the x-axis again, the speed is nearly zero. This value correspond to S_∞ . The value of S_I for the greywacke (agg.4) occurs at $1.3E-05$ and S_∞ is equal to $2.6E-05$. The crushed gravel 17, with a lower velocity (already mentioned), also shows a lower value for $S_I = 1.1E-05$ and $S_\infty = 2.5E-05$. For all eighteen aggregates, the ratio of S_I/S_∞ was about 0.40-0.50. But there is a particularity. It can be seen that the higher k_1 , the higher S_I & S_∞ . This seems to be valid for all aggregates except 4 and 17. Obviously a proportional correlation is suggested. The ratio of k_1/S_∞ for aggregate 4 leads to $3.4E-07/2.6E-05 = 13E-02$. The crushed gravel 17 leads to a ratio of $1.2E-02$. Therefore, aggregate 1 has a value of $6.7E-03$ and the andesite (agg.7) $6.4E-03$. The values for the andesite are taken from the calculation parameters, because its curve is difficult to find in **Fig. 11**. What does this mean? It shows that above a critical velocity dS/dt here $2.8E-07$ (maximum value of agg.1) one or more cracks in the cement matrix were initiated. The gel leads into the crack volume as an additional space and the pressure is decreased. Thus no more pressure for expansion progress is available, and the values of S_I & S_∞ (at x-axis) get smaller. But it also means that the "crack free" values of S_I & S_∞ could be calculated like $S_\infty = k_1/6.5E-03$. The loss of modulus of elasticity (also determined, but not shown here) confirms the appearance of cracks.

The value dS/dt represents the ASR sensitivity, because the influence of the SiO_{2exc} solubility was eliminated (2). It represents a basic reactivity, which every aggregate has. The larger this value, the more expansion should be expected in CPT. Usually the basic reactivity would have to be equal for all aggregates, but dS/dt ranges from $3.0E-08$ till $3.4E-07$. Why are some aggregates more or less sensitive? Is there any important value missing? Well, until now the open porosity was neglected. It can be assumed that k_1 , S_I and S_∞ are functions of p_o . It is clear, that all three values must increase if the porosity decreases. The less pore volume for ASR gel is available, the more deleterious the ASR will be. As expected **Fig. 12** shows the important influence of the open porosity. On the x-axis, the weighted porosity is converted in a volume of open pores each specimen has. It varies between 1.65 and 8.54 in³ (27 and 140 cm³). The open porosity here is the average value of several measurements. Therefore, a power function was determined. For all three variables, the degree of certainty lies above 83% under considering of all aggregates. The gravels show a wide range of solubility values. If the gravels are not taken into account the degree of certainty is about 95%.

The next step will be the validation of the achieved expertise. The **Fig. 13** shows the calculated expansion curves for the andesite (agg.7), greywacke (agg.4) and the rounded gravels (agg.2 & 16). The comparison between the calculation and the experimental results shows a quite good agreement. The andesite 7, rounded gravel 16 and 2 can be predicted very good. The calculated expansion speed of the greywacke (agg.4) is lower than the experimental data, but the maximum expansion is higher. The calculated expansion here is the elastic expansion

without any cracks. The prediction leads to the result that the greywacke 4 is very sensitive to ASR. While gravel 2 is medium sensitive, aggregate 16 and andesite 7 are innocuous.

FURTHER RESEARCH

This method should be further developed to improve the accuracy. It was shown that the open porosity decreases the ASR expansion. On the other hand, the bigger the porosity the bigger the surface available for alkalis. The porosity of the cement paste can be an additional value too. The open porosity should take into account these facts. At this moment, multiple dissolution samples of one aggregate type are investigated to detect the procedural error of dissolution experiments. Crushed aggregates show a better repeatability than gravels. This might be the reason for the lower degree of certainty of k_1 , S_I and S_∞ (**Fig. 12**).

It might be possible to reduce the assessment time smaller than 56 d, by early predicting the SiO_{2exc} dissolution curves. In the future the algorithm will be tested to more aggregate fractions e.g. 0.63/0.87 (16/22). Currently new expansion data are obtained from concrete specimens with lower alkali content. This might be helpful to reduce the ASR potential even from aggregates like greywacke 4 or crushed gravel 17. This model approach should be able to consider SCM's and their effect to dissolution and concrete expansion too.

This method can also be applied to other international concrete ASR assessment tests (e.g. ASTM C1567).

CONCLUSIONS

Based on the results of this experimental investigation, the following conclusions are drawn:

1. Solubility values (SiO_{2exc}) and physical parameters (p_o) of aggregate grains have a great influence on the reaction behavior of concrete prisms and can be used as a data set for calculation of the expansion curves. With this method the additional influences of SiO_{2exc} and p_o can be separated.
2. Based on these data a phenomenological model is developed to describe the expansion behavior of a variety of different aggregates.
3. The model can display the ASR sensitivity of aggregates and distinguish between innocuous, medium and highly reactive. The assessment time for a standard ASR CPT test could be significantly reduced from 9 to 2 months.
4. It was shown, that crushed gravel grains have a higher ASR sensitivity than the rounded ones. Crushing a gravel in tests should be avoided.

REFERENCES

1. Hill, S., "Zur direkten Beurteilung der Alkaliempfindlichkeit präkambrischer Grauwacken aus der Lausitz anhand deren Silicium- und Aluminiumlösungsverhalten", PhD Thesis, TU Cottbus, 2004, 168 pp.
2. Huenger, K.-J., "The contribution of quartz and the role of aluminum for understanding the AAR with Greywacke", Cement and Concrete Research, V. 37, No. 8, 2007, pp. 1193-1205.
3. Chappex, T., and Scrivener, K., "The influence of aluminium on the dissolution of amorphous silica and its relation to alkali silica reaction", Cement and concrete research, V. 42, 2012, pp. 1645-1649.
4. Bachmann, R., "Über das Zusammenspiel chemischer und physikalischer Gesteinsparameter zum besseren Verständnis des Ablaufs einer schädigenden Alkali-Kieselsäure-Reaktion", PhD Thesis, TU Cottbus, 2014, 203 pp.
5. Kronemann, J., "Untersuchung der zeitlichen Abhängigkeit von Löseprozessen in hochalkalischen Lösungen zur Charakterisierung der Alkaliempfindlichkeit von Gesteinskörnungen", PhD Thesis, TU Cottbus-Senftenberg, 2015.
6. DAfStb-Richtlinie - Vorbeugende Maßnahmen gegen schädigende Alkalireaktion im Beton (Alkali-Richtlinie); 10/2013; Beuth Verlag

7. Charpin, L.; Ehrlacher A., “A computational linear elastic fracture mechanics-based model for alkali-silica reaction”, *Cement and concrete research*, V. 42, 2012, pp. 613-625.
8. Santos, R. et al., “Study of the structural behaviour of Pirapora dam affected by alkali-aggregate reaction”, ICAAR 2016, Sao Paulo
9. BS EN 1097-6:2013 - Tests for mechanical and physical properties of aggregates. Determination of particle density and water absorption; British Standard; July 2013
10. Jawed, J.; Skalny, J. and Young, J.F., “Hydration of Portland Cement”, *Structure and performance of cements*, 1984.
11. Kondo, R.; Ueda, S., “Kinetics and mechanism of the hydration of cement”, *Intern. Congress on the Chemistry of Cement*, 1968, vol.II, pp. 203-255.
12. Sessner, R.; Pirner, J., “Stoffliche, mathematische und technologische Grundlagen für CAD-CAM-Lösungen der Fertigungsstufen 2 und 5”, PhD Thesis, 1989.
13. Peter Deuffhard, Folkmar Bornemann: Numerische Mathematik. Band 2: Gewöhnliche Differentialgleichungen. 2. vollständige überarbeitete und erweiterte Auflage. de Gruyter, Berlin 2002, ISBN 3-11-017181-3.

TABLES AND FIGURES

List of Tables:

Table 1 – Investigated aggregates

Table 2 – OPC composition and properties

Table 3 – Standard concrete mixture design for fog chamber [6]

List of Figures:

Fig. 1 – BTU-SP Test results with different aggregates

Fig. 2 – Method of mod. BTU-Test

Fig. 3 – mod. BTU-Test results with two aggregates

Fig. 4 – Pictures of four aggregates used

Fig. 5 – Evolutionary function with reaction- and diffusion period

Fig. 6 – Open porosity of the aggregates

Fig. 7 – Solubility of $\text{SiO}_{2\text{exc}}$ according to mod. BTU-Test

Fig. 8 – Results of the modified BTU-Test

Fig. 9 – Experimental expansion results from the CPT

Fig. 10 – Results of regression analysis, dS/dt against time

Fig. 11 – Results of regression analysis, dS/dt against $S(t)$

Fig. 12 – Important influence of open porosity on model parameters

Fig. 13 – Model validation

Table 1 – Investigated aggregates

	no.
rounded gravel	1, 2, 9, 10, 11, 13*, 16*
crushed gravel	12*, 15, 17*
rhyolite	3, 6, 8, 14
greywacke	4, 18
quartzite	5
andesite	7

* The gravels 12/13 and 16/17 come from an identical origin material. The only difference is the grain shape.

Table 2 – OPC composition and properties

	value
Specific gravity, lb/ft ³ (g/cm ³)	195.40 (3.13)
Blaine fineness, ft ² /lb (cm ² /g)	1684.44 (3450)
Loss of ignition, %	2.02
SiO ₂ , %	20.02
Al ₂ O ₃ , %	4.98
CaO, %	61.31
MgO, %	3.57
SO ₃ , %	3.07
Na ₂ O, %	0.17
K ₂ O, %	1.39
Na ₂ O _{eq} , %	1.09
MnO, %	0.09
TiO ₂ , %	0.25
Fe ₂ O ₃ , %	3.24

Table 3 – Concrete mixture design for fog chamber [6]

	value
OPC, lb/ft ³ (kg/m ³)	24.97 (400.0)
Water, lb/ft ³ (kg/m ³)	11.24 (180.0)
Aggregate Sand 0/0.08 (0/2)	30.0 vol.-%
Aggregate 0.08/0.31 (2/8)	40.0 vol.-%
Aggregate 0.31/0.63 (8/16)	30.0 vol.-%
Air pores	1.50 vol.-%

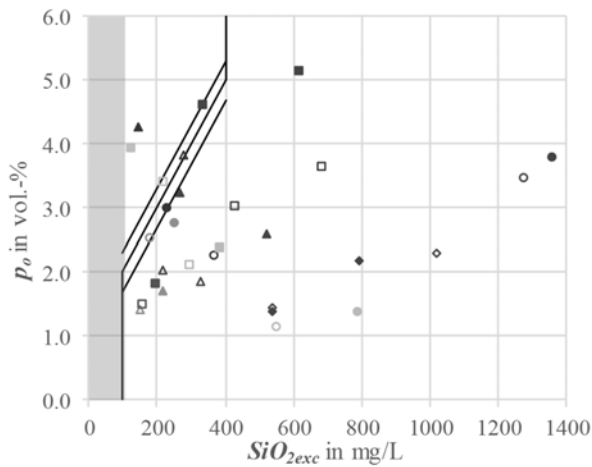


Fig. 1 – BTU-SP Test results with different aggregates

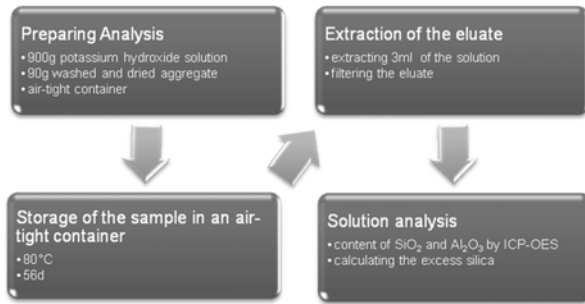


Fig. 2 – Method of mod. BTU-Test

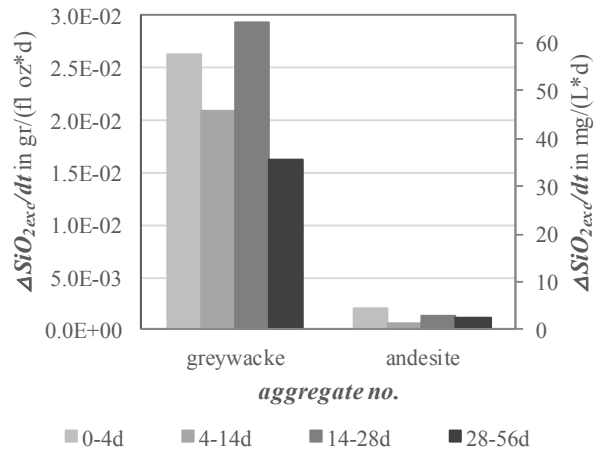


Fig. 3 – mod. BTU-Test results with two aggregates



Fig. 4 – Pictures of four aggregates used

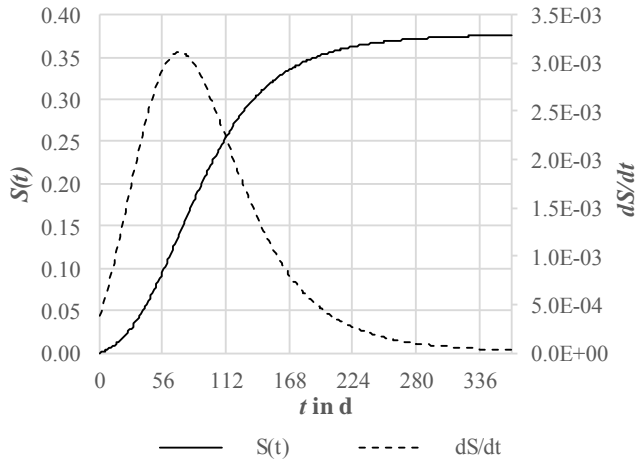


Fig. 5 – Evolutionary function with reaction- and diffusion period

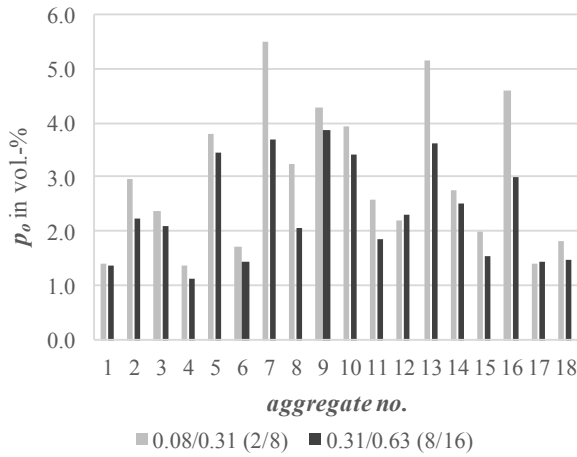


Fig. 6 – Open porosity of the aggregates

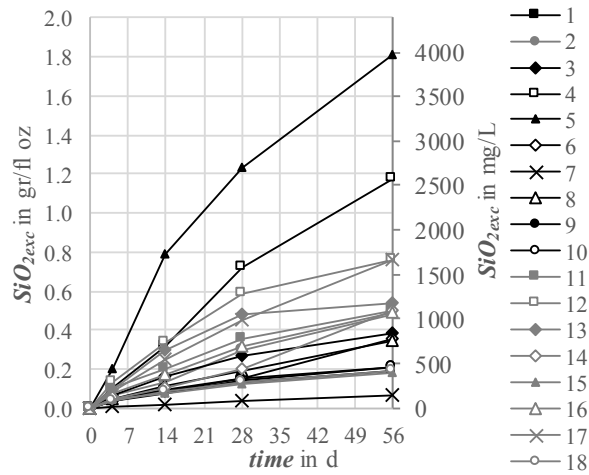


Fig. 7 – Solubility of SiO_{2,exc} according to mod. BTU-Test

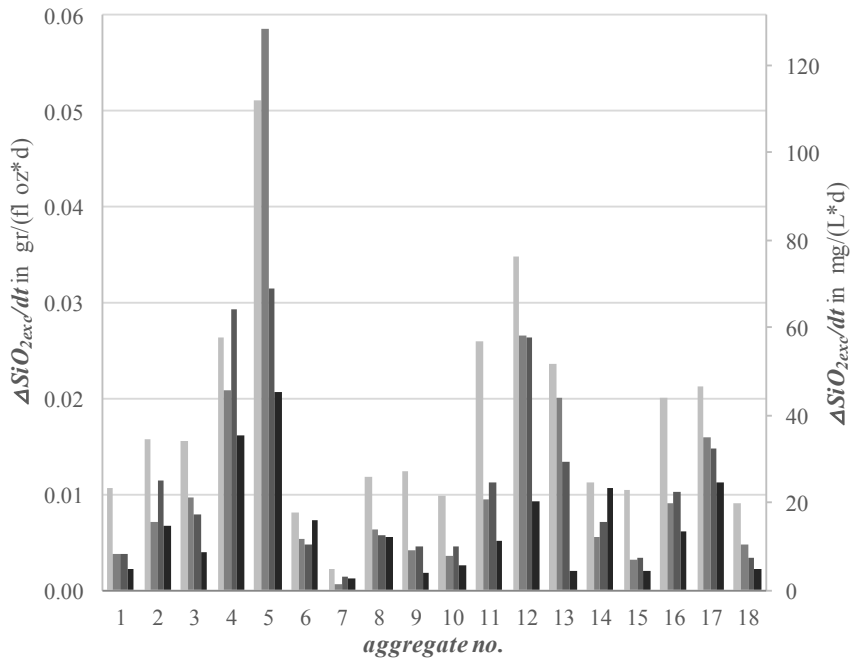


Fig. 8 – Results of the modified BTU-Test

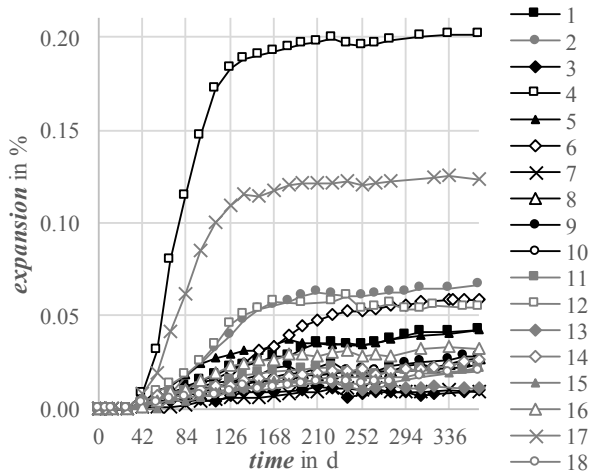


Fig. 9 – Experimental expansion results from the CPT

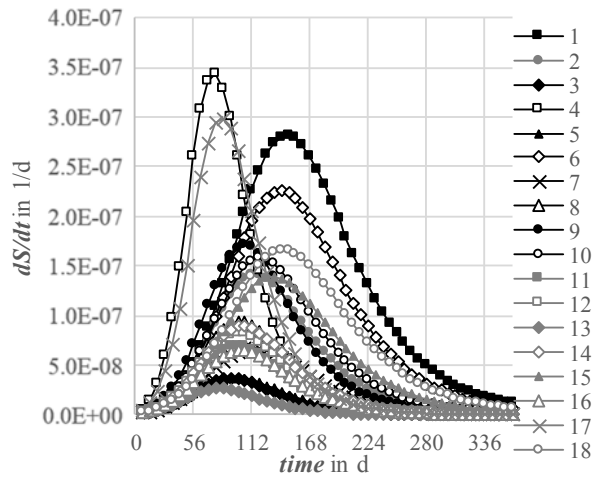


Fig. 10 – Results of regression analysis, dS/dt against time

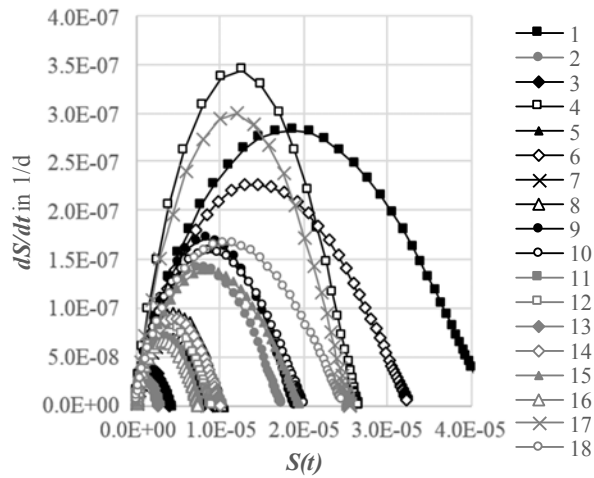


Fig. 11 – Results of regression analysis, dS/dt against $S(t)$

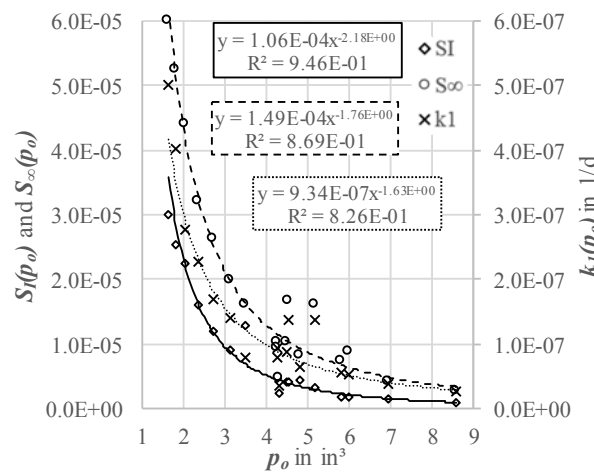


Fig. 12 – Important influence of open porosity on model parameters

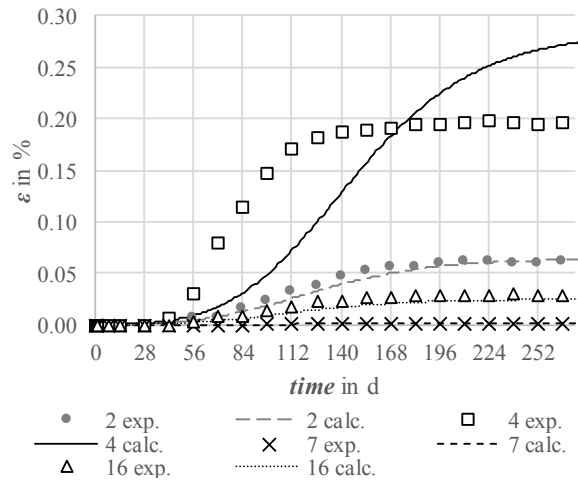


Fig. 13 – Model validation